

Measurement of $\psi(3770)$ parameters

V. V. Anashin^a, V. M. Aulchenko^{a,b}, E. M. Baldin^{a,b}, A. K. Barladyan^a, A. Yu. Barnyakov^a, M. Yu. Barnyakov^a, S. E. Baru^{a,b}, I. Yu. Basok^a, O. L. Beloborodova^{a,b}, A. E. Blinov^a, V. E. Blinov^{a,c}, A. V. Bobrov^a, V. S. Bobrovnikov^a, A. V. Bogomyagkov^{a,b}, A. E. Bondar^{a,b}, A. R. Buzykaev^a, S. I. Eidelman^{a,b}, D. N. Grigoriev^a, Yu. M. Glukhovchenko^a, V. V. Gulevich^a, D. V. Gusev^a, S. E. Karnaev^a, G. V. Karpov^a, S. V. Karpov^a, T. A. Kharlamova^{a,b}, V. A. Kiselev^a, V. V. Kolmogorov^a, S. A. Kononov^{a,b}, K. Yu. Kotov^a, E. A. Kravchenko^{a,b}, V. F. Kulikov^{a,b}, G. Ya. Kurkin^{a,c}, E. A. Kuper^{a,b}, E. B. Levichev^{a,c}, D. A. Maksimov^a, V. M. Malyshev^a, A. L. Maslennikov^a, A. S. Medvedko^{a,b}, O. I. Meshkov^{a,b}, S. I. Mishnev^a, I. I. Morozov^a, N. Yu. Muchnoi^a, V. V. Neufeld^a, S. A. Nikitin^a, I. B. Nikolaev^{a,b}, I. N. Okunev^a, A. P. Onuchin^{a,c}, S. B. Oreshkin^a, I. O. Orlov^a, A. A. Osipov^a, S. V. Peleganchuk^a, S. G. Pivovarov^{a,c}, P. A. Piminov^a, V. V. Petrov^a, A. O. Poluektov^a, V. G. Prisekin^a, A. A. Ruban^a, V. K. Sandyrev^a, G. A. Savinov^a, A. G. Shamov^{a,*}, D. N. Shatilov^a, B. A. Shwartz^{a,b}, E. A. Simonov^a, S. V. Sinyatkin^a, A. N. Skrinsky^a, V. V. Smaluk^a, A. V. Sokolov^a, A. M. Sukharev^a, E. V. Starostina^{a,b}, A. A. Talyshev^{a,b}, V. A. Tayursky^{a,b}, V. I. Telnov^{a,b}, Yu. A. Tikhonov^{a,b}, K. Yu. Todyshev^{a,b,*}, G. M. Tumaikin^a, Yu. V. Usov^a, A. I. Vorobiov^a, A. N. Yushkov^a, V. N. Zhilich^a, V. V. Zhulanov^{a,b}, A. N. Zhuravlev^{a,b}

^a*Budker Institute of Nuclear Physics, Siberian Div., Russian Acad. Sci., 630090, Novosibirsk, Russia*

^b*Novosibirsk State University, 630090, Novosibirsk, Russia*

^c*Novosibirsk State Technical University, 630092, Novosibirsk, Russia*

Abstract

We report the final results of a study of the $\psi(3770)$ meson using a data sample collected with the KEDR detector at the VEPP-4M electron-positron collider. The data analysis takes into account interference between the resonant and nonresonant $D\bar{D}$ production, where the latter is related to the nonresonant part of the energy-dependent form factor F_D . The vector dominance approach and several empirical parameterizations have been tried for the nonresonant $F_D^{NR}(s)$.

Our results for the mass and total width of $\psi(3770)$ are

$$M = 3779.2^{+1.8}_{-1.7}{}^{+0.5}_{-0.7}{}^{+0.3}_{-0.3} \text{ MeV},$$

$$\Gamma = 24.9^{+4.6}_{-4.0}{}^{+0.5}_{-0.6}{}^{+0.2}_{-0.9} \text{ MeV},$$

where the first, second and third uncertainties are statistical, systematic and model, respectively. For the electron partial width two possible solutions have been found:

$$(1) \quad \Gamma_{ee} = 154^{+79}_{-58}{}^{+17}_{-9}{}^{+13}_{-25} \text{ eV},$$

$$(2) \quad \Gamma_{ee} = 414^{+72}_{-80}{}^{+24}_{-26}{}^{+90}_{-10} \text{ eV}.$$

Our statistics are insufficient to prefer one solution to another. The solution (2) mitigates the problem of non- $D\bar{D}$ decays but is disfavored by potential models.

It is shown that taking into account the resonance–continuum interference in the near-threshold region affects resonance parameters, thus the results presented can not be directly compared with the corresponding PDG values obtained ignoring this effect.

1. Introduction

The preceding Letter of this volume is devoted to the measurement of the $\psi(2S)$ meson parameters in the KEDR experiment performed during energy scans from 3.67 to 3.92 GeV at the VEPP-4M e^+e^- collider. In this Letter we describe the application of the developed tools to the measurement of $\psi(3770)$ parameters omitting details common for $\psi(2S)$ and $\psi(3770)$.

Since the discovery of the $\psi(3770)$, seven experiments contributed to the determination of its parameters, nevertheless the

situation with the mass, total width and electron partial width is still not clear.

The incomplete compilation of results reported on $\psi(3770)$ mass is presented in Table 1. It does not include the results of Refs. [12, 13] with the analysis of the $e^+e^- \rightarrow D\bar{D}$ data of BES [14] and the $e^+e^- \rightarrow D\bar{D}\gamma$ data of Belle [15] in which the $\psi(3770)$ electron width has been fixed in the fits causing a mass bias. In addition, the bin size in Belle data around $\psi(3770)$ seems too large for a simple center-of-bin fitting. These works encouraged us to employ the vector dominance model in the analysis [11].

The values presented form three partially overlapping clus-

*Corresponding authors, e-mails:
shamov@inp.nsk.su, todyshev@inp.nsk.su

ters. The first one with $\langle M \rangle = 3772.5 \pm 0.4$ MeV comes from the analyses in which interference between resonant and nonresonant $D\bar{D}$ production has been ignored [1, 2, 3, 5, 6, 7]. In addition, the analyses assumed the simplest shape of nonresonant $D\bar{D}$ -cross section similar to that for point-like pseudoscalars in QED. The statistical uncertainty in this case is small (in [7] the influence of $\psi(4040)$ and higher ψ 's included in the analysis increases the $\psi(3770)$ mass uncertainty). The second cluster of $B \rightarrow D\bar{D}K$ analyses [4, 8, 9] has $\langle M \rangle = 3775.6 \pm 2.3$ MeV (the result of [4] is not included because of its uncertain status). The third, highest mass, cluster is formed by the analyses accounting for interference [10, 11] and gives $\langle M \rangle = 3777.3 \pm 1.3$ MeV.

As was mentioned in Section 5.2 of the previous Letter, taking into account the resonance-continuum interference is essential for a determination of the $\psi(3770)$ parameters. A close $D\bar{D}$ production threshold significantly increases the importance of that. A consideration of the interference effects is one of the primary goals of this experiment¹.

If interference is ignored in a fit of the measured $D\bar{D}$ or multihadron cross section, a bias appears in the growing continuum contribution that causes a bias in the resonance amplitude and a shift of the mass value. The signs of these effects depend on the relative position of the interference peak and dip. The $D\bar{D}$ cross section at the threshold is fixed at zero, therefore the weights of the more distant data points in a fit are larger than those of the less distant ones. Evidence for a dip after the $D\bar{D}$ cross section maximum is visible in all published data with large enough statistics (see, for example, Fig. 1 of Ref. [6]), therefore, the artificial mass shift should be negative (undercounted events move the resonance peak to the left). That is exactly what we observe analyzing the published mass results.

If the result on mass of [4] is ignored, the $\psi(3770)$ mass value obtained in B decays does not contradict neither to 3772.5 nor 3777.3 MeV. The interference of the resonant and nonresonant $D\bar{D}$ yields also takes place in this case but the relation between them can differ from that in e^+e^- collisions, besides, the interference effect can be partially compensated by subtraction of the combinatorial background. Thus, the intermediate mass value does not seem surprising.

Below we briefly describe the theoretical basis of the analysis performed, enter some details concerning the analysis procedure and not covered in the preceding Letter, present the results on the $\psi(3770)$ parameters and discuss their systematic uncertainties and model dependence.

2. Multihadron cross section in the vicinity of $\psi(3770)$

A few approaches can be employed to determine the resonance parameters using a multihadron cross section data. In the Ref. [6] the fit of the R ratio was performed, in the Ref. [16] the efficiency-corrected cross section was analyzed. There are many different sources of multihadron events such as the $\psi(2S)$ and $\psi(3770)$ production, the light quark production etc., thus

Table 1: Incomplete compilation of results on $\psi(3770)$ mass.

Analysis	$M_{\psi(3770)}$ [MeV]	Comments
MARK-I [1]	3774.1 ± 3	$e^+e^- \rightarrow$ hadrons ^(a)
DELCO [2]	3772.1 ± 2	$e^+e^- \rightarrow$ hadrons ^(a)
MARK-II [3]	3766.1 ± 2	$e^+e^- \rightarrow$ hadrons ^(a)
Belle [4]	$3778.4 \pm 3.0 \pm 1.3$	$B \rightarrow D^0\bar{D}^0K^+$ ^(b)
KEDR [5]	$3773.5 \pm 0.9 \pm 0.6$	$e^+e^- \rightarrow$ hadrons ^(c)
BES-II [6]	$3772.4 \pm 0.4 \pm 0.3$	$e^+e^- \rightarrow$ hadrons ^(a)
BES-II [7]	3772.0 ± 1.9	$e^+e^- \rightarrow$ hadrons
Belle[8]	$3776.0 \pm 5.0 \pm 4.0$	$B \rightarrow D^0\bar{D}^0K^+$
BaBar [9]	$3775.5 \pm 2.4 \pm 0.5$	$B \rightarrow D\bar{D}K$
BaBar [10]	$3778.8 \pm 1.9 \pm 0.9$	$e^+e^- \rightarrow D\bar{D}\gamma$ ^(d)
KEDR [11]	$3778.0 \pm 1.6 \pm 0.7$	$e^+e^- \rightarrow$ hadrons ^(c,d)

^(a) — omitted in the latest PDG edition

^(b) — the result on $\mathcal{B}(B \rightarrow D^0\bar{D}^0K^+)$ is superseded by [8]

^(c) — preliminary results reported at various conferences

^(d) — interference between resonant and nonresonant $D\bar{D}$ production is taken into account

the variation of the net detection efficiency in the whole experiment range can exceed 20% [17]. The calculation of the net efficiency implies knowledge of the resonance parameters and accounting for the interference effects, therefore an iterative analysis is required. In this work we fit the observed multihadron cross section not corrected for the detection efficiency which allows iterations to be avoided.

2.1. Observed cross section and D -meson form factor

In the energy range from slightly below the $\psi(2S)$ peak to slightly above the $D\bar{D}\pi$ threshold the variation of the light quark contribution to R (R_{uds}) is small, so that the multihadron cross section observed in the experiment can be written as

$$\begin{aligned} \sigma_{mh}^{\text{obs}} = & \varepsilon_{\psi(2S)} \sigma_{\psi(2S)}^{\text{RC}} + \varepsilon_{J/\psi} \sigma_{J/\psi}^{\text{RC}} + \varepsilon_{\tau\tau} \sigma_{\tau\tau}^{\text{RC}} + \sigma_{uds}^{\text{emp}} + \\ & \varepsilon_{D^+D^-} \sigma_{D^+D^-}^{\text{RC}} + \varepsilon_{D^0\bar{D}^0} \sigma_{D^0\bar{D}^0}^{\text{RC}} + \varepsilon_{nD\bar{D}} \mathcal{B}_{nD\bar{D}} \sigma_{\psi(3770)}^{\text{RC}} + \quad (1) \\ & \sigma_{D\bar{D}\pi}^{\text{emp}} \end{aligned}$$

where σ^{RC} 's are theoretical cross sections, ε 's are corresponding detection efficiencies, and σ^{emp} 's are terms treated empirically as described below. The RC superscript means that the cross section has been corrected for initial state radiation (ISR) effects, $nD\bar{D}$ stands for the direct $\psi(3770)$ decay to light hadrons, the other (super/sub)scripts seem self-explanatory, $\mathcal{B}_{nD\bar{D}}$ is a branching fraction. All detection efficiencies explicitly entering Eq. (1) can be kept energy independent with sufficient accuracy for the event selection criteria employed (see Sec. 3.1).

The first four terms have no peculiarities in the whole energy range of the experiment, while the last four are responsible for the excess of the cross section in the $\psi(3770)$ region.

¹The result of [5] was obtained solely to check consistency with the previous measurements.

The fourth term of Eq. (1) corresponding to the light quark contribution can be scaled as $1/s^{1-\delta}$ where a relatively small parameter δ is due to the energy dependence of the detection efficiency and radiative corrections. Possible variation of R_{uds} can also contribute to δ . This term can be easily removed from the consideration in the fit of the cross section provided that the δ value is known. The $D\bar{D}\pi$ cross section can be treated as a small correction. We took it into account using the approximately known shape and an additional fit parameter.

Calculations for $\sigma_{\psi(2S)}^{RC}$ and $\sigma_{\tau\tau}^{RC}$ are described in the preceding Letter, a small contribution of the J/ψ tail was calculated similarly to the $\psi(2S)$ one, for the $D\bar{D}$ production cross section (here and below D stands for D^+ or D^0) one has

$$\sigma_{D\bar{D}}^{RC}(W) = \int z_{D\bar{D}}(W' \sqrt{1-x}) \sigma_{D\bar{D}}(W' \sqrt{1-x}) \times \mathcal{F}(x, W'^2) G(W, W') dW' dx, \quad (2)$$

where $\mathcal{F}(x, s)$ is the probability to lose a fraction of s in the initial state radiation [18], $G(W, W')$ describes a distribution of the total collision energy, which can be assumed to be Gaussian with an energy spread σ_W .

For the charged mode (D^+D^-) the factor $z_{D^+D^-}$ describing the Coulomb interaction between the mesons produced [19] is taken according to Sommerfeld-Sakharov [20, 21, 22]:

$$z_{D^+D^-} = \frac{\pi\alpha/\beta_{D^+}}{1 - \exp(-\pi\alpha/\beta_{D^+})} \times \theta(W - 2m_{D^+}). \quad (3)$$

For the neutral mode ($D^0\bar{D}^0$) there is no such interaction, thus

$$z_{D^0\bar{D}^0} = 1 \times \theta(W - 2m_{D^0}), \quad (4)$$

the step functions $\theta(W - 2m_D)$ are shown explicitly to simplify some expressions below.

The cross section $\sigma_{D\bar{D}}$ can be expressed via the form factor F_D and D -meson velocity in the c.m.system β_D :

$$\sigma_{D\bar{D}}(W) = \frac{\pi\alpha^2}{3W^2} \beta_D^3 |F_D(W)|^2, \quad \beta_D = \sqrt{1 - 4m_D^2/W^2}. \quad (5)$$

To determine the parameters of resonances above the $D\bar{D}$ threshold, their amplitudes should be separated in F_D :

$$F_D(W) = \sum_i F_D^{R_i}(W) e^{i\phi_i} + F_D^{NR}(W), \quad (6)$$

where ϕ_i is the phase of the i -th resonance R_i relative to F_D^{NR} .

For the resonance with the partial widths Γ_{ee} and $\Gamma_{D\bar{D}}$ and the total width $\Gamma(W)$, one has a Breit-Wigner amplitude

$$F_D^R(W) = \frac{6 \sqrt{(\Gamma_{ee}/\alpha^2) (\Gamma_{D\bar{D}}(W)/\beta_D^3)} W}{M^2 - W^2 - iM\Gamma(W)} \quad (7)$$

(the vacuum polarization factor is included in Γ_{ee}).

Considering $\Gamma(M)$ as a nominal resonance width and introducing the sum of the branching fractions to all non- $D\bar{D}$ modes $\mathcal{B}_{nD\bar{D}}$, one obtains the energy-dependent $D\bar{D}$ partial width

$$\Gamma_{D\bar{D}}(W) = \frac{(M/W) z_{D\bar{D}}(W) d_{D\bar{D}}(W) \cdot \Gamma(M) \cdot (1 - \mathcal{B}_{nD\bar{D}})}{z_{D^0\bar{D}^0}(M) d_{D^0\bar{D}^0}(M) + z_{D^+D^-}(M) d_{D^+D^-}(M)} \quad (8)$$

in line with the PDG prescriptions (p. 808 of Ref. [23]). Here $d_{D^+D^-}$ and $d_{D^0\bar{D}^0}$ are the Blatt-Weisskopf damping factors for a vector resonance [24]:

$$d_{D\bar{D}} = \frac{\rho_{D\bar{D}}^3}{\rho_{D\bar{D}}^2 + 1}, \quad \rho_D = q_D R_0, \quad (9)$$

where R_0 represents the meson radius and q_D is the c.m. momentum of the meson $q_D = \beta_D W/2$. The partial width dependence according to Eq. (8) corresponds to the approach of Ref. [19]. Its simplified form was used in the experiments [1, 2, 3]. The approach is somewhat different from that employed in Refs. [6, 7] by BES which does not lead to noticeable changes of the $\psi(3770)$ parameters.

The $D\bar{D}\pi$ cross section entering (1) as a small correction can be calculated with sufficient accuracy using

$$\sigma_{D\bar{D}\pi}(W) = \frac{\pi\alpha^2}{3W^2} \beta_{D\bar{D}\pi}^3 |F_{D\bar{D}\pi}|^2, \quad (10)$$

$$\beta_{D\bar{D}\pi} = \sqrt{(1 - (m_{D^+} + m_D)^2/W^2)(1 - (m_{D^+} - m_D)^2/W^2)}.$$

The quantity $F_{D\bar{D}\pi}$ is treated as a fit parameter.

2.2. Nonresonant D -meson form factor

The nonresonant part of the form factor can be written as

$$F_D^{NR}(W) = \frac{1}{|1 - \Pi_0(W)|} f_D(W) \quad (11)$$

with $f_D(W) = 1$ for point-like particles. Here Π_0 is the vacuum polarization operator except the contributions of all resonances which are written separately in (6). We remind that the full polarization operator is calculated using the total cross section of $e^+e^- \rightarrow hadrons$ that already includes all resonances, therefore use of the full operator Π instead of Π_0 in the nonresonant amplitude leads to double counting of the resonances and thus incorrect values of the leptonic widths (see also the discussion in Sec. 5.3 of the preceding Letter).

There are no precise theoretical predictions for $F_D^{NR}(W)$. The model-independent result can be obtained using the expansions of $\text{Re } F_D^{NR}(W)$ and $\text{Im } F_D^{NR}(W)$ at the point $W = M$ with the coefficients free in the fit. Our statistics are not sufficient for that, thus we have to rely on some model or use a pure empirical approach as in Ref. [10] by BaBar also taking into account the resonance-continuum interference.

The most certain prediction of the form factor can be obtained with an application of the Vector Dominance Model (VDM) to charm production. Standard VDM assumes that the inclusive cross section $e^+e^- \rightarrow hadrons$ at low energy is saturated by the interfering contributions of the limited number of vector mesons. A similar assumption can be accepted for the inclusive $e^+e^- \rightarrow c\bar{c}$ cross section and its exclusive modes such as $e^+e^- \rightarrow D\bar{D}$. The VDM-like analysis of the R ratio in the energy range of $W = 3.7 \div 5$ GeV has been performed by BES in Ref. [7], where the light quark contribution R_{uds} was calculated using pQCD. The work cited accounts for $\psi(3770)$,

$\psi(4040)$, $\psi(4160)$ and $\psi(4415)$ resonances but does not account for a possible contribution of $\psi(2S)$ decays to $D\bar{D}$ above the threshold. Studies of this contribution Refs. [12, 13] include a theoretical consideration and some analysis of the $D\bar{D}$ cross section measured by BES as well as by BELLE. In this work we employ VDM in a simplified form

$$F_D^{NR}(W) = F_D^{\psi(2S)}(W) + F_0, \quad (12)$$

where F_0 is a real constant representing the contributions of the $\psi(4040)$ and higher ψ 's. The $\psi(2S)$ contribution to the $D\bar{D}$ form factor $F_D^{\psi(2S)}$ was calculated using Eq. (7) with the $D^0\bar{D}^0$ and D^+D^- partial widths defined similarly to Eq. (8) with a specific value of the effective radius R_0 . The value of $\Gamma_{D\bar{D}}^{\psi(2S)}(M_{ref}) = \Gamma_{D^+D^-}^{\psi(2S)}(M_{ref}) + \Gamma_{D^0\bar{D}^0}^{\psi(2S)}(M_{ref})$ at some reference point M_{ref} , as well as the constant F_0 , should be obtained from the data fit ($M_{ref} = 3778$ MeV was used). The partial width ratio $\Gamma_{D^0\bar{D}^0}^{\psi(2S)}/\Gamma_{D^+D^-}^{\psi(2S)}$ is presumably close to that of $\psi(3770)$.

To evaluate the model dependence of the $\psi(3770)$ parameters we tried a few nonresonant form factor parameterizations, which do not assume vector dominance. The most popular empirical parameterization is probably exponential:

$$f_D = \exp(-q_D^2/a^2),$$

where q_D is the c.m. momentum [25]. It is well motivated far above the threshold but has few parameters to describe the low energy region. Instead of it we used

$$f_D = -\frac{g_q}{(1 + a_q q_D^2 + b_q q_D^4)^n} \quad (n = 0.5, 1). \quad (13)$$

The minus sign is chosen to match the $\psi(2S)$ dominance expectations. In the case $n = 0.5$, $b_q = 0$, the nonresonant cross section acquires the Blatt-Weisskopf factor (9) with $R_0 = a_q$. The case $n = 1$ corresponds to a more rapid form factor fall. Use of two parameters a_q and b_q allows us to take into account in the limited energy range the increase of the $D\bar{D}$ cross section described by the $G(3900)$ structure in the Ref. [10]. Alternatively, the dependence on $W - m_D$

$$f_D = -\frac{g_W}{1 + a_W(W - 2m_D) + b_W(W - 2m_D)^2} \quad (14)$$

and combined dependences

$$f_D = -\frac{g_{qW}}{(1 + a_{qW}(W - 2m_D) + b_{qW}q_D^2)^n} \quad (15)$$

were considered.

To check validity of the $\psi(2S)$ domination hypothesis in Eq. (12) the following parameterizations were used:

$$f_D = \frac{g_m}{a_m - W} \left(1 + \frac{i b_m \beta_D^n}{a_m - W} \right) \quad (n = 0, 1, 3), \quad (16)$$

where β_D is the D -meson velocity. They are expansions of the Breit-Wigner amplitude with the mass a_m treated as a free parameter, the values of n correspond to different assumptions on $\Gamma(W)$ dependence. In case of $\psi(2S)$ dominance the fitted value of a_m would be close to $M_{\psi(2S)}$.

3. Data analysis

3.1. Detection efficiency determination

To perform a fit of the observed multihadron cross section with Eq. (1), it is necessary to know six detection efficiencies explicitly entering the equation and the detection efficiency ε_{uds} implicitly contained in the term σ_{uds}^{emp} related to the continuum light quark production. They were determined from Monte Carlo simulation. The efficiency $\varepsilon_{nD\bar{D}}$ enters Eq. (1) in the product with the non- $D\bar{D}$ branching fraction $\mathcal{B}_{nD\bar{D}}$, which is rather uncertain. That allows one to assume $\varepsilon_{nD\bar{D}} \approx \varepsilon_{\psi(2S)}$.

The event selection criteria, which are different for 2004 and 2006 scans, and the procedure of the detection efficiency determination for the $\psi(2S)$ decay simulation are described in detail in the preceding Letter. The tuned version of the BES generator [26] was employed to the obtained $\psi(2S)$ detection efficiency in the vicinity of the peak. The same version of the generator with parameters optimal for $\psi(2S)$ simulation was used to simulate the $\psi(2S)$ and J/ψ tails and the continuum uds production. To simulate $e^+e^- \rightarrow D\bar{D}$ events, $D\bar{D}$ pairs were first generated with the proper angular distribution. Decays of D mesons were simulated using the routine *LU2ENT* of the *JETSET 7.4* package [27]. The decay tables of *JETSET* were updated according to those of the PDG review [23].

Table 2: Detection efficiency for the processes of interest and its variation in the experiment energy range $\Delta W \approx 200$ MeV.

Process	ε_{2004}	ε_{2006}	$\Delta\varepsilon/\varepsilon, \%$
D^+D^-	0.75 ± 0.02	0.84 ± 0.02	$+1.0 \pm 0.3$
$D^0\bar{D}^0$	0.74 ± 0.02	0.81 ± 0.02	$+1.0 \pm 0.3$
$\psi(2S)$	0.63 ± 0.01	0.72 ± 0.01	-0.1 ± 0.1
J/ψ	0.50 ± 0.02	0.60 ± 0.02	-0.2 ± 0.1
uds	0.55 ± 0.02	0.69 ± 0.02	$+2.1 \pm 0.5$

The detection efficiencies for the processes of interest and their energy variations are presented in Table 2. The systematic uncertainties of the efficiencies $\varepsilon_{J/\psi}$ and ε_{uds} were estimated by variation of JETSET parameters preserving the mean value of the charged multiplicity. The systematic uncertainties on $\varepsilon_{D^+D^-}$ and $\varepsilon_{D^0\bar{D}^0}$ were found modifying the decay branching fractions of D -mesons within uncertainties quoted in the PDG tables.

3.2. Fitting of data

The observed multihadron cross section was fitted as a function of W with the expression (1) using some assumptions about the behaviour of the nonresonant form factor F_D^{NR} . The details on the likelihood calculation can be found in the preceding Letter. The following additional constraint was applied

$$\left| \frac{F_{D^+}^{NR}(W_{ref})}{F_{D^0}^{NR}(W_{ref})} \right|^2 = \frac{\sigma_{D^+D^-}(W_{ref})}{\sigma_{D^0\bar{D}^0}(W_{ref})} = r_{00}^+, \quad (17)$$

with the reference mass $W_{ref} = 3773$ MeV not far from the observed cross section maximum. The value $r_{00}^+ = 0.776_{-0.025}^{+0.028}$ [28]

was used. The world average values were also used for the J/ψ mass, total and electronic width. The total width of $\psi(2S)$ was fixed at the value of 296 ± 9 keV obtained in the preceding Letter. The meson radii of Eq. (9) were fixed at 1 fm and 0.75 fm for $\psi(3770)$ and $\psi(2S)$, respectively (Refs. [29, 30, 31]). Since the experimental results on the non- $D\bar{D}$ fraction of $\psi(3770)$ decays $\mathcal{B}_{nD\bar{D}}$ are controversial and theory expects it to be small, we performed the fits with $\mathcal{B}_{nD\bar{D}} = 0$ and 0.16 and assigned variation of the parameters to the systematic uncertainties.

The light quark contribution was parameterized as

$$\sigma_{uds}^{emp} = \varepsilon_{uds} (1 + \delta_{uds}^{RC}) \bar{R}_{uds} \left(\frac{M_{\psi(2S)}^2}{s} \right)^{1-\delta} \sigma_{\mu\mu}^B(M_{\psi(2S)}), \quad (18)$$

where δ_{uds}^{RC} is a radiative correction of about 0.12, \bar{R}_{uds} is a light quark contribution to the R ratio averaged over the experiment energy range and $\sigma_{\mu\mu}^B$ in a Born level dimuon cross section. The values of δ_{uds}^{RC} and ε_{uds} are constants corresponding to $W = M_{\psi(2S)}$. The parameter δ was fixed at 0.187 ± 0.046 with the uncertainties dominated by that of the detection efficiency variation presented in Table 2. The detailed discussion can be found below in Sec. 4.4.

A simultaneous fit of three scans has been performed. Each scan has its own free parameters (the energy spread σ_W and \bar{R}_{uds}) and has other free parameters common for all three scans. Among them are the mass $M_{\psi(2S)}$, the product of the electron width and the branching fraction of its decay to hadrons $\Gamma_{ee} \times \mathcal{B}_{hadr}$ for $\psi(2S)$; the mass M , the total width Γ , the electron width Γ_{ee} and the interference phase ϕ for $\psi(3770)$. The $D\bar{D}\pi$ contribution was tuned using the free parameter $F_{D\bar{D}\pi}$. The non-resonant form factor has been controlled by either the free parameters $\Gamma_{D\bar{D}}^{\psi(2S)}(M_{ref})$ (the $\psi(2S)$ partial width above the $D\bar{D}$ threshold) and F_0 (constant term of the form factor) or by three parameters g, a, b defined in Eqs. (13), (14), (15) and (16). The last but not least free parameter was the interference phase ϕ . The total number of free parameters was either 15 or 16.

The parameters controlling the nonresonant form factor behaviour have strongly correlated asymmetric statistical errors. Instead of them we present below the value of the nonresonant $D\bar{D}$ cross section at the resonance peak $\sigma_{D\bar{D}}^{NR}(M)$ and its error obtained in fits with modified sets of free parameters (e.g., the $(F_0, \Gamma_{D\bar{D}}^{\psi(2S)})$ pair was replaced with the $(F_0, \sigma_{D\bar{D}}^{NR})$ one).

The observed multihadron cross section for the scans is presented in Fig. 1. The curve represents the vector dominance fit. The resulting values of $\psi(2S)$ parameters agree very well with those obtained fitting the narrow energy range around $\psi(2S)$ (previous Letter). The difference in the mass values is 2 keV, the variation of the $\Gamma_{ee} \times \mathcal{B}_h$ product is about 0.3%. As a consistency check, we estimate \bar{R}_{uds} for the three scans. The fitted values are $2.33 \pm 0.10, 2.25 \pm 0.09$ and 2.31 ± 0.06 . The weighted average $\bar{R}_{uds} = 2.300 \pm 0.046 \pm 0.108$ ($\chi^2/N_{Dof} = 0.49/2$) agrees well with a similar value 2.262 ± 0.122 published by BES in Ref. [32] and does not contradict to the result of the BES measurement [33]: $R = 2.14 \pm 0.01 \pm 0.07$ at $W = 3.65$ GeV.

The excess of the multihadron cross section in the $\psi(3770)$ region is shown in Fig. 2. To calculate the excess, the terms

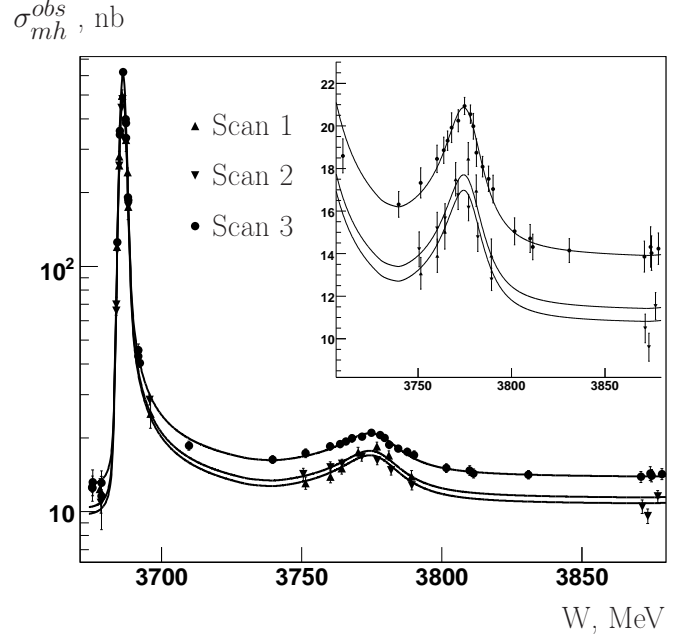


Figure 1: The observed multihadron cross section as a function of the c.m. energy for the three scans. The curves are the results of the vector dominance fit. The detection efficiencies and the energy spreads for the scans differ.

1–4 of Eq. (1) obtained by the vector dominance fit were subtracted from the measured cross section at each point, the residuals were corrected for the detection efficiency calculated by weighting the fit terms 5–8. These terms of the fits are presented with the curves. The ignored-interference fit and the fits with the anomalous line shapes from Ref. [16] are presented for comparison.

3.3. On ambiguity of resonance parameters

It is known that for two interfering resonances the ambiguity can appear in the resonance amplitudes and the interference phase. A detailed study of that issue can be found in Ref. [34]. In the case of two resonances with constant widths complete degeneration occurs: one obtains the identical cross sections for two combinations of the amplitudes and phase at the same values of the mass and width.

For the energy-dependent widths there is no complete degeneration, however, the likelihood function has local maxima on the amplitude-phase plane at slightly different mass and width values. A similar situation occurs when a resonance interferes with a varying continuum.

In our case the typical difference in equivalent χ^2 values of the two local minima is very small, $-2\Delta \ln(L) \simeq 0.02$, thus a certain solution can not be chosen. The variation of mass and width for possible solutions is small and neglected below.

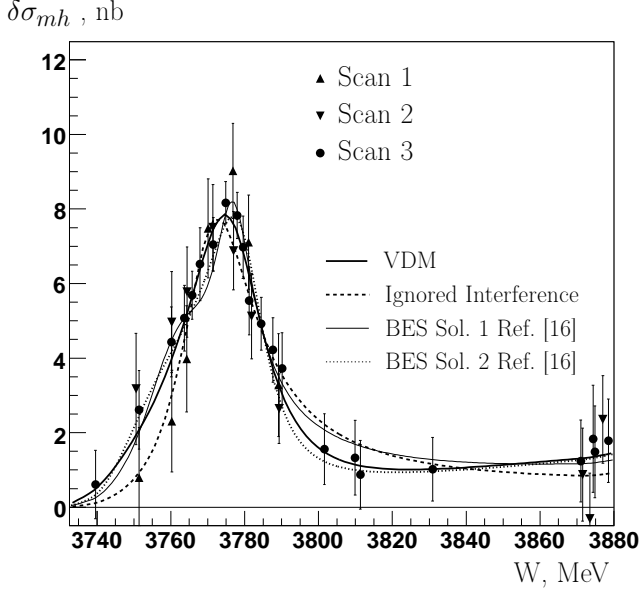


Figure 2: Excess of the multihadron cross section in the $\psi(3770)$ region. The curves show relevant parts of the fits. The error bars correspond to the uncertainty of the measured multihadron cross section. All data are corrected for the detection efficiency which is different in the three scans. See the detailed explanation in the text.

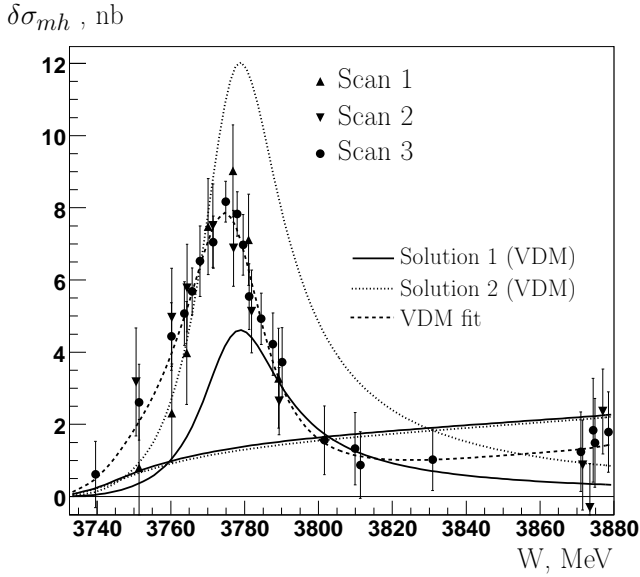


Figure 3: Excess of the multihadron cross section in the $\psi(3770)$ region. Solid and short-dashed curves correspond to two VDM solutions. Resonant and non-resonant parts are presented separately.

4. Results of analysis

4.1. $\psi(3770)$ parameters assuming vector dominance

In Table 3 we compare the $\psi(3770)$ parameters obtained under the assumption of $\psi(2S)$ dominance in the nonresonant form factor for two possible solutions with those extracted from

the ignored-interference fit and the current world average values. The small corrections to residual background given below in Table 5 of Sec. 4.3 are not applied to results of the fit. The continuum $D\bar{D}$ cross section $\sigma_{D\bar{D}}^{NR}$ is given without the radiative correction factor of about 0.75. The values of the mass and the electron width for the ignored-interference fit are in good agreement with the world average ones, while the value of the total width deviates from the average one by 1.5 standard deviation. That is probably due to the statistical fluctuation that occurred at the three points of the first scan (see Fig. 2).

Taking into account the resonance–continuum interference in $D\bar{D}$ production improves the chi-square of the fits from 91.1/73 to 74.8/71. The phase of the $\psi(3770)$ amplitude relative to the nonresonant form factor is about 171 and 240 degrees for the first and second solution, respectively. The nonresonant form factor has a negative real part and a small imaginary one. At the $\psi(3770)$ peak $\psi(2S)$ contributes approximately 70% to the total value of the nonresonant form factor. If the resonance–continuum interference is ignored, the total width is not substantially affected, however, the mass shift of about -6.0 MeV appears as well as dramatical change of the value and error of the electron width. The nonresonant $D\bar{D}$ cross section in this case is underestimated as was discussed in the introduction.

A large splitting of the Γ_{ee} values is expected in the near-threshold region. Let us illustrate that with an example of the area method of the Γ_{ee} determination discussed soon after the J/ψ discovery [35]. The electron width is proportional to the area under the resonance curve

$$\Gamma_{ee} = k \frac{M^2}{6\pi^2} \int \sigma_{res}(W) dW \quad (19)$$

(the coefficient k is equal to unity for the energy-independent total width), therefore the following expression can be obtained in absence of radiative corrections for the case when the continuum cross section is small compared to the resonant one:

$$\Gamma_{ee}^{i.i.} \approx \Gamma_{ee} \left(1 + \frac{\alpha}{3} \sqrt{\frac{R_C(M)}{B_{ee}}} \sin \phi \right) + \frac{2\alpha\sqrt{B_{ee}}}{3\pi} M \cos \phi \times \int \frac{(W-M) \sqrt{\Gamma(M)\Gamma(W)} \sqrt{R_C(W)} dW}{(W-M)^2 + \Gamma(W)^2/4} \quad (20)$$

Here α is the fine structure constant, R_C is the continuum contribution to R , B_{ee} – the e^+e^- branching fraction and ϕ is the interference phase. The continuum cross section $\propto (\sqrt{R_C})^2$ is neglected.

The left part of (20) corresponds to the area under the measured curve (Γ_{ee} is obtained ignoring the interference), the right part has three terms corresponding to the area under the resonance curve itself (the true Γ_{ee}), the curve due to the imaginary part of the resonance amplitude (it is also proportional to Γ_{ee}) and the area of the interference wave due to the real part of the amplitude.

Far enough from the threshold, R_C and $\Gamma(W)$ are almost constant and the integral is suppressed proportionally to Γ/M . However, for a varying R_C and an asymmetric $\Gamma(W)$ near the threshold, it grows up to $0.02 \div 0.15 \sqrt{R_C(M)}$ depending on the

Table 3: $\psi(3770)$ fit results for the vector dominance compared to the ignored-interference case.

Solution	M , MeV	Γ , MeV	Γ_{ee} , eV	ϕ , degrees	$\Gamma_{D\bar{D}}^{\psi(2S)}$, MeV	F_0	$\sigma_{D\bar{D}}^{NR}$, nb	$P(\chi^2)$, %
1	$3779.3^{+1.8}_{-1.7}$	$25.3^{+4.4}_{-3.9}$	160^{+78}_{-58}	170.7 ± 16.7	$12.9^{+18.5}_{-11.8}$	$-4.8^{+3.0}_{-3.6}$	1.83 ± 0.96	35.7
2	$3779.3^{+1.8}_{-1.6}$	$25.3^{+4.6}_{-4.0}$	420^{+72}_{-80}	239.6 ± 8.6	$11.5^{+16.5}_{-10.5}$	$-4.9^{+3.3}_{-3.7}$	1.71 ± 0.86	35.7
i.i.	3773.3 ± 0.5	$23.3^{+2.5}_{-2.2}$	249^{+25}_{-22}	-	-	-	$0.07^{+0.09}_{-0.07}$	7.5
PDG [23]	3772.92 ± 0.35	27.3 ± 1.0	265 ± 18	-	-	-	-	-

 Table 4: $\psi(3770)$ fits results for alternative assumptions on the nonresonant form factor f_D .

Model	Mass, total width and $P(\chi^2)$			Solution 1 (smaller ϕ)			Solution 2 (larger ϕ)		
Equation	M , MeV	Γ , MeV	$P(\chi^2)$, %	ϕ , degrees	Γ_{ee} , eV	$\sigma_{D\bar{D}}^{NR}$, nb	ϕ , degrees	Γ_{ee} , eV	$\sigma_{D\bar{D}}^{NR}$, nb
(13) n=1	$3779.1^{+2.0}_{-1.6}$	$24.4^{+5.0}_{-3.6}$	32.7	167.6 ± 16.0	146^{+66}_{-48}	1.82 ± 0.76	243.1 ± 9.5	417^{+75}_{-65}	1.76 ± 0.73
(13) n=0.5	$3779.0^{+1.7}_{-1.6}$	$25.5^{+3.0}_{-3.5}$	33.1	172.2 ± 17.3	172^{+241}_{-66}	1.59 ± 0.86	241.0 ± 15.6	418^{+76}_{-65}	1.55 ± 0.66
(14)	$3779.0^{+2.1}_{-1.9}$	$24.4^{+5.1}_{-3.7}$	32.7	167.5 ± 21.3	145^{+83}_{-49}	2.09 ± 0.87	243.1 ± 9.5	418^{+76}_{-74}	2.02 ± 0.86
(15) n=1	$3779.0^{+2.0}_{-1.7}$	$24.4^{+5.1}_{-3.7}$	32.7	167.4 ± 20.4	145^{+68}_{-49}	2.14 ± 0.88	243.0 ± 9.6	422^{+75}_{-74}	2.07 ± 0.86
(15) n=0.5	$3779.0^{+1.7}_{-1.6}$	$25.2^{+4.2}_{-2.8}$	33.1	172.2 ± 21.6	171^{+68}_{-65}	1.81 ± 0.88	241.3 ± 11.9	419^{+75}_{-68}	1.76 ± 0.85
(16) n=0	3779.6 ± 2.0	25.3 ± 6.6	31.9	200.4 ± 14.7	137 ± 87	2.20 ± 0.93	230.3 ± 33.0	461 ± 73	2.47 ± 1.37
(16) n=1	3779.6 ± 1.9	25.3 ± 6.3	31.8	176.1 ± 16.6	154 ± 113	2.14 ± 0.91	239.4 ± 14.7	433 ± 74	1.96 ± 0.96
(16) n=3	3779.1 ± 1.7	25.2 ± 4.4	32.9	126.0 ± 15.8	139 ± 88	1.89 ± 0.90	282.0 ± 16.9	501 ± 89	2.54 ± 0.91

assumptions about the energy dependence of Γ and R_C . The closeness to the threshold increases the influence of the interference effects by an order of magnitude. The coefficient preceding $\cos \phi$ in Eq.(20) is about 18 keV in the $\psi(3770)$ case, the fits give $R_C(M) \simeq 0.3$ with a 40÷50% statistical uncertainty. Together these circumstances make the area method inapplicable to $\psi(3770)$. A fit of the cross section is obviously not so sensitive to taking interference into account, nevertheless a splitting of about 260 eV in Table 3 does not seem surprising.

The resonant and continuum cross sections for the two VDM solutions are presented in Fig. 3. The choice of the true solution is essential for determination of the non- $D\bar{D}$ branching fraction of $\psi(3770)$. At the c.m. energy of 3773 MeV the resonance cross section of $3.8^{+1.9}_{-1.4}$ nb for the first solution and $9.9^{+1.7}_{-1.9}$ nb for the second one should be compared with the non- $D\bar{D}$ cross section, which is $1.08 \pm 0.40 \pm 0.15$ nb according to BES [36] and $-0.01 \pm 0.08^{+0.41}_{-0.30}$ according to CLEO [37]. The branching fraction of about 28% for the first solution seems unreasonable, however, that can not be considered as a strong argument in favor of the second solution until improvement in the non- $D\bar{D}$ cross section accuracy.

4.2. Model dependence of results

To evaluate the model dependence of the $\psi(3770)$ parameters and to check the validity of the vector dominance approach,

the fits were performed with the alternative assumptions about the nonresonant form factor $f_D(W)$ described in Sec. 2.2. The results of the fits are presented in Table 4. A few other assumptions were also tried.

The amplitude-phase ambiguity was found in all cases considered. For each fit we assigned the number 1 to the solution with a smaller phase value, while the alternative solution got the number 2. The electron width for the first solution was always smaller than that of the second one and the values for two clusters did not overlap.

The results obtained assuming q^2 dependence of the nonresonant form factor as in Eq.(13) almost coincide with those for $W-m_D$ and mixed dependence in Eq. (14) and (15) because of the relatively narrow energy range of the experiment.

The mass parameter a_m of the parameterizations of Eq. (16) $n = 0, 1, 3$ lies between the $\psi(2S)$ mass and the $D\bar{D}$ threshold confirming the $\psi(2S)$ dominance. Accepting that the $\psi(3770)$ parameters corresponding to the vector dominance model are the most reliable, we derive the following estimates for the model dependence: $\delta M = {}^{+0.3}_{-0.3}$ MeV, $\delta \Gamma = {}^{+0.2}_{-0.9}$ MeV for both solutions and $\delta \Gamma_{ee} = {}^{+13}_{-25} ({}^{+90}_{-10})$ eV, $\delta \sigma_{D\bar{D}}^{NR} = {}^{+0.4}_{-0.2} ({}^{+0.8}_{-0.2})$ nb for solutions 1 (2), respectively. The maximum deviation of parameters from the VDM results was taken. The definition of the phase ϕ with Eq.(6) allows its model-to-model variation, however, the difference with VDM exceeds the statistical uncertainty only in

the cases (16) $n = 0, 3$ due to a relatively large imaginary part of the nonresonant form factor fitted in these cases.

We also fitted our data with the anomalous line shapes considered in the Ref. [16] by BES where a sum of two noninterfering Breit-Wigner cross sections and a sum of two destructively interfering amplitudes were referred to as Solution 1 and Solution 2, respectively. The parameters of the amplitudes were fixed according to Ref. [16], the two free parameters were introduced to correct the general normalization and the shift of the energy scale. The $\psi(3770)$ scale correction averaged for two shapes is 1.042 ± 0.052 at the energy shift of 0.92 ± 0.51 MeV which demonstrates rather good consistency of KEDR and BES data in general. The chi-square probabilities $P(\chi^2)$ are 25.4 and 30.3% for the solutions 1 and 2, respectively, compared to 35.7% for the vector dominance fit. Both shapes provide a better description of the data than the single Breit-Wigner amplitude not interfering with the nonresonant one (“i.i.” case in Table 3) due to increase of the resonant yield below 3765 MeV. In addition, the destructive interference in Solution 2 reduces the resonant yield above 3790 MeV but that does not improve significantly the general fit quality because of the growth of the peculiarity in the 3765–3780 MeV energy region absent in our case. Accounting for the resonance–continuum interference with a Breit-Wigner resonance amplitude provides the best fit of our data although with our statistics we can not exclude the shape anomaly reported in Ref [16]. It is worth noting that interference of the $\psi(3770)$ structure with the continuum $D\bar{D}$ amplitude should be considered for any shape assumed.

4.3. Correction for residual background

The residual machine background is about 2% of the observed uds cross section for the scan of 2006 and five times less for the scans of 2004 (Sec. 6.3 of the preceding Letter). The estimated numbers of background events are 445 ± 97 and 24 ± 7 , respectively, whereas the total number of multihadron events selected above the $D\bar{D}$ threshold is 33678.

To evaluate the impact of the residual background on the resulting fit parameters, the background admixture was changed in a controllable way. To do so, we prepared a few samples of background events passing some loose selection criteria but rejected by the multihadron ones. At each data point i the number of multihadron events N_i^{mh} was replaced with $N_i^{mh} + f \cdot N_i^{bg}$, where N_i^{bg} is the number of events in the background sample. The fits with the modified number of events show that the variations of all fit parameters are proportional to f in the case $|f| \cdot N_i^{bg} \ll N_i^{mh}$. Selecting the negative f values at which the total number of subtracted events matches the expected background admixture and taking into account a small detection efficiency change, we obtain the corrections for the fit parameters presented in Table 5. The systematic uncertainties quoted include those of the background admixture estimate and the variation of corrections obtained using different background samples.

4.4. Systematic uncertainties

The main sources of systematic uncertainty in $\psi(3770)$ parameters are listed in Table 6.

Table 5: Correction to fit results compensating the bias due to the background admixture.

Correction	Solution 1	Solution 2
δM , MeV	-0.06 ± 0.06	-0.06 ± 0.06
$\delta \Gamma$, MeV	-0.4 ± 0.3	-0.4 ± 0.3
$\delta \Gamma_{ee}$, %	-3.9 ± 2.9	-1.5 ± 1.1
$\delta \sigma_{D\bar{D}}^{NR}$, %	$+1.5 \pm 0.5$	$+1.5 \pm 0.5$
$\delta \bar{R}_{uds}^{2004}$, %	-0.5 ± 0.3	-0.5 ± 0.3
$\delta \bar{R}_{uds}^{2006}$, %	-2.5 ± 1.0	-2.5 ± 1.0

When the resonance-continuum interference is taken into account, the multihadron cross section becomes rather sensitive to the non- $D\bar{D}$ fraction of $\psi(3770)$ decays. It was varied from zero to 0.16 as was mentioned in Section 3.2. The variations of the $\psi(3770)$ mass and total width were 0.3 and 0.1 MeV, respectively. The shift of the electron width was +8.8% for the first solution and -2.3% for the second one.

The uncertainty on the R_0 value used to specify the energy-dependent width (8), (9) of about 25% (Refs. [30, 31]) leads to these of 0.3 MeV both in the mass and total width. When the interference is ignored, the sensitivity to R_0 variations reduces by a factor of 3.

The uncertainties due to that of the branching fraction ratio for $D^0\bar{D}^0$ and D^+D^- are about 0.1 MeV for the mass and total width. Approximately the same uncertainties are obtained because of the D meson masses. The estimates were obtained by variation of the values within their errors quoted by PDG.

To estimate uncertainties due to the inaccuracy of the $D\bar{D}\pi$ cross section treatment at the edge of the energy range of the experiment, we used two methods: shrinking of the fit range and assumption of the linear dependence on the D -meson c.m. velocity instead of the cubical one in Eq. (10). The latter corresponds to variation of the effective interaction radius R_0 for $D\bar{D}\pi$ states from zero to infinity. The variations of the mass, total width and electron width do not exceed 0.15 MeV, 0.05 MeV and 1%, respectively.

The systematic uncertainties due to the energy dependence of the detection efficiencies shown in Table 2 can be neglected in all cases except ϵ_{uds} . The latter together with the energy dependence of the radiative correction factor and possible R_{uds} variation determine the power in the expression (18) used to parameterize the light quark contribution to the multihadron cross section. The radiative correction factor $1 + \delta_{uds}^{RC} = 1.125 \pm 0.022$ was calculated according to Ref. [18] using the vacuum polarization data compilation by the CMD-2 group reviewed in Ref. [38]. The error quoted includes the uncertainty of the detection efficiency dependence on the mass of the hadronic system produced via ISR and that of the vacuum polarization data. We explicitly considered the J/ψ tail in the cross section (1), thus the correction factor is 14–9% less than that used in Ref. [32] and its variation in the experiment energy range

Table 6: Systematic uncertainties on the $\psi(3770)$ mass, total width and electron partial width. For the latter the uncertainties of two solutions are presented where different. The uncertainty on the nonresonant $D\bar{D}$ cross section is also presented.

Source	M [MeV]	Γ [MeV]	Γ_{ee} [%]	$\sigma_{D\bar{D}}^{NR}$ [%]
Theoretical uncertainties and external data precision				
$\mathcal{B}_{nD\bar{D}}$	+0.0 -0.5	+0.0 -0.2	+8.8 / +0 -0	+0 -12.
R_0 value in $\Gamma(W)$	0.3	0.3	2.	1.5
$\Gamma_{D^0\bar{D}^0}/\Gamma_{D^+D^-}$	0.1	0.1	0.4	0.8
D, \bar{D} masses	0.06	0.04	0.3	0.5
$D\bar{D}\pi$ cross section	0.15	0.05	1.	2.
Detector and accelerator related uncertainties				
Det. efficiency variation	0.03	0.04	2.4	5.
Hadronic event selection	0.3	0.3	3.	5.
Residual background	0.06	0.3	2.9	3.
Luminosity measurement	0.1	0.1	2.	2.
Beam energy	0.03	–	–	–
<i>Sum in quadrature</i>	+0.48 -0.69	+0.54 -0.58	+10.5 / +5.7 -5.7 / -6.1	+8. -14.

does not reach 0.1%. The precise R measurements at $W = 3.07$ and 3.65 MeV [33] do not indicate essential R_{uds} variation, thus we concluded that the uds efficiency variation dominates in the uncertainty of the power $1-\delta$. Performing the fits with different values of δ we evaluated the uncertainty of the $\psi(3770)$ parameters as 0.03 MeV, 0.04 MeV and 2.4% for the mass, total width and electron width, respectively. Compared to that, the energy dependence of $\varepsilon_{D\bar{D}}$ gives only a 0.5% bias of the electron width and a few keV shifts of the mass and total width.

The sensitivity of the mass and width to the criteria of the multihadron event selection was checked by changing cuts on the energy deposited in the calorimeter and conditions on the number of tracks. The results were stable within 0.3 MeV. The detection efficiency uncertainty due to inaccuracy of the D -meson decay ratios [23] used for the simulation contributes 2% to the electron width uncertainty. The dependence on the choice of the selection criteria increases it up to 3%. The sensitivity to the event selection criteria is partially due to the influence of the residual background. We ignore that and treat the background correction as an independent uncertainty source which makes the uncertainty estimates more conservative.

Uncertainties due to the luminosity measurement instability are less than 0.1 MeV for the mass and width. The accuracy of the absolute luminosity measurements discussed in the preceding Letter contributes less than 2% to the electron width uncertainty. The uncertainty on $\psi(3770)$ mass due to the beam energy determination does not exceed 30 keV.

5. Summary

The parameters of the $\psi(3770)$ meson have been measured using the data collected with the KEDR detector at the VEPP-4M e^+e^- collider. Interference of resonant and nonresonant production essential in the near-threshold region has been taken into account.

Our final results on the mass and width of $\psi(3770)$ are:

$$M = 3779.2^{+1.8}_{-1.7} {}^{+0.5}_{-0.7} {}^{+0.3}_{-0.3} \text{ MeV},$$

$$\Gamma = 24.9^{+4.6}_{-4.0} {}^{+0.5}_{-0.6} {}^{+0.2}_{-0.9} \text{ MeV},$$

The corrections applied to the fit results are listed in Table 5. The third error arises from the model dependence. It was estimated comparing the results obtained under the assumption of vector dominance in the D -meson form factor (quoted values) and under a few alternative assumptions which do not imply vector dominance. The quoted model errors do not include possible deviations of the resonance shape from the Breit-Wigner one with usual assumptions about the total width energy dependence, which are predicted, e.g., in the coupled-channel model [29].

The result on the $\psi(3770)$ mass agrees with that by BaBar also taking into account interference (Ref. [10]) and is significantly higher than all results obtained ignoring this effect. The mass values obtained studying B -meson decays by BaBar [9] and Belle [8] are lower but do not contradict to our measurement.

We got two possible solutions for the $\psi(3770)$ electron partial width and the radiatively corrected nonresonant $D\bar{D}$ cross section at the mass of $\psi(3770)$:

$$(1) \Gamma_{ee} = 154^{+79}_{-58} {}^{+17}_{-9} {}^{+13}_{-25} \text{ eV}, \quad \sigma_{D\bar{D}}^{NR} = 1.4 \pm 0.7^{+0.1}_{-0.2} {}^{+0.3}_{-0.2} \text{ nb},$$

$$(2) \Gamma_{ee} = 414^{+72}_{-80} {}^{+24}_{-26} {}^{+90}_{-10} \text{ eV}, \quad \sigma_{D\bar{D}}^{NR} = 1.3 \pm 0.7^{+0.1}_{-0.2} {}^{+0.6}_{-0.2} \text{ nb}.$$

The phase shifts of the $\psi(3770)$ amplitude relative to the negative nonresonant amplitude are 171 ± 17 and 240 ± 9 degrees for solutions (1) and (2), respectively.

Most of potential models support the first solution and can barely tolerate the second one. The increase of the $\psi(3770)$ mass according to the BaBar and KEDR measurements implies the decrease of the $2S$ - $1D$ mixing used in potential models to rise the electron width value above 100 eV (Refs. [39, 40, 41, 42] and the reviews [43, 44]). The correct choice of the true solution is extremely important for a determination of the non- $D\bar{D}$ fraction of $\psi(3770)$ decays.

Because of the large uncertainty the solution (1) does not contradict formally to the previously published results, which do not take the interference effect into account, the solution (2) is only two standard deviations higher than the current world average. However, the qualitative consideration and numerical estimates confirm that the impact of the resonance–continuum interference on the resulting electron width value is large, therefore the resonance parameters obtained taking into account interference can not be directly compared with the corresponding values obtained ignoring this effect.

Acknowledgments

We greatly appreciate permanent support of the staff of the experimental, accelerator and electronics laboratories while preparing and performing this experiment. Stimulating discussions with V. P. Druzhinin are acknowledged.

This work was partially supported by the Ministry of Education and Science of the Russian Federation and grants Sci.School 6943.2010.2, RFBR 10-02-00695, 11-02-00112, 11-02-00558.

References

References

- [1] P. A. Rapidis *et al.*, Phys. Rev. Lett. **39** (1977) 526.
- [2] W. Bacino *et al.*, Phys. Rev. Lett. **40** (1978) 671.
- [3] R. H. Shindler *et al.*, Phys. Rev. D **21** (1980) 2716.
- [4] K. Abe *et al.* [Belle Collaboration], Phys. Rev. Lett. **93** (2004) 051803.
- [5] K. Y. Todyshev *et al.* [KEDR Collaboration], PoS **HEP2005** (2006) 115.
- [6] M. Ablikim *et al.* [BES Collaboration], Phys. Lett. B **652** (2007) 238.
- [7] M. Ablikim *et al.* [BES Collaboration], eConf **C070805** (2007) 02 [Phys. Lett. B **660** (2008) 315].
- [8] J. Brodzicka *et al.* [Belle Collaboration], Phys. Rev. Lett. **100** (2008) 092001.
- [9] B. Aubert *et al.* [BABAR Collaboration], Phys. Rev. D **77** (2008) 011102.
- [10] B. Aubert *et al.*, Phys. Rev. D **76** (2007) 111105(R).
- [11] K. Y. Todyshev [KEDR Collaboration], PoS **ICHEP2010** (2010) 218.
- [12] H. B. Li, X. S. Qin and M. Z. Yang, Phys. Rev. D **81** (2010) 011501.
- [13] Y. J. Zhang and Q. Zhao, Phys. Rev. D **81** (2010) 034011.
- [14] M. Ablikim *et al.* [BES Collaboration], Phys. Lett. B **668** (2008) 263.
- [15] G. Pakhlova *et al.* [Belle Collaboration], Phys. Rev. D **83** (2011) 011101
- [16] M. Ablikim *et al.*, Phys. Rev. Lett. **101** (2008) 102004.
- [17] D. Zhang *et al.*, Phys. Rev. D **74** (2006) 054012
- [18] E. A. Kuraev and V. S. Fadin, Sov. J. Nucl. Phys. **41** (1985) 466.
- [19] M. B. Voloshin, Prog. Part. Nucl. Phys. **61** (2008) 455.
- [20] A. Sommerfeld, Atombau und Spektrallinien, vol. **II** (Vieweg, Braunschweig, 1939).
- [21] A. D. Sakharov, Sov. Phys. JETP **18** (1948) 631.
- [22] K. A. Milton, I. L. Solovtsov, Mod. Phys. Lett. A **16** (2001) 2213.
- [23] K. Nakamura *et al.*, J. Phys. G **37** (2010) 075021.
- [24] J.M. Blatt and V.F. Weisskopf, Theoretical Nuclear Physics, Wiley, New York, (1952).
- [25] A. De Rújula *et al.*, Phys. Rev. Letters **37** (1976) 398.
- [26] J.C. Chen *et al.*, Phys. Rev. D **62** (2000) 034003.
- [27] T. Sjostrand and M. Bengtsson, Comp. Phys. Comm. **43** (1987) 367.
- [28] Q. He *et al.*, Phys. Rev. Lett. **95** (2005) 121801
- [29] E. Eichten *et al.*, Phys. Rev. D **21** (1980) 203.
- [30] W. Buchmuller and S. H. H. Tye, Phys. Rev. D **24** (1981) 132.
- [31] S. Godfrey and N. Isgur, Phys. Rev. D **32**, (1985) 189.
- [32] M. Ablikim *et al.* [BES Collaboration], Phys. Lett. B **641** (2006) 145.
- [33] M. Ablikim *et al.* [BES Collaboration], Phys. Lett. B **677** (2009) 239
- [34] A. D. Bukin, arXiv:0710.5627 [physics.data-an].
- [35] J. D. Jackson and D. L. Scharre, Nucl. Instrum. Meth. **128** (1975) 13.
- [36] M. Ablikim *et al.* [BES Collaboration], Phys. Lett. B **659** (2008) 74.
- [37] D. Besson *et al.* [CLEO Collaboration], Phys. Rev. Lett. **96** (2006) 092002 [Erratum-ibid. **104** (2010) 159901] [arXiv:hep-ex/0512038].
- [38] S. Actis *et al.*, Eur. Phys. J. C **66** (2010) 585.
- [39] A. M. Badalian and I. V. Danilkin, Phys. Atom. Nucl. **72** (2009) 1206.
- [40] S. F. Radford and W. W. Repko, Phys. Rev. D **75** (2007) 074031.
- [41] P. González *et al.*, Phys. Rev. D **68** (2003) 034007.
- [42] J. M. Richard, Z. Phys. C **4** (1980) 211.
- [43] N. Brambilla *et al.*, Eur. Phys. J. C **71** (2011) 1534.
- [44] N. Brambilla *et al.* [Quarkonium Working Group], arXiv:hep-ph/0412158.